

Image Fusion Based on WRV and NHM Rules for Medical Digital Image in Contourlet Domain

Juan WANG¹, Siyu LAI², Borjer T.H³

¹Computer School, China West Normal University
Nanchong, 637002, China

²Imaging Department, North Sichuan Medical College
Nanchong, 637000, China

³Information Institute for Geographic Engineering in ABB Communication Corporation
Patras, 138682, Greece
wjuan0712@126.com



*Journal of Digital
Information Management*

ABSTRACT: *With the rapid development of medical information management, there are an increasing number of medical digital images, and clinicians need to integrate comprehensive multi-source images to make an accurate diagnosis of a patient. To improve the ability to understand the fused information of multi-source medical images, a technique for image fusion based on weighted regional variance (WRV) and neighborhood homogeneous measurement (NHM) rules was proposed in this article. First, the source images were decomposed in multi-scale and multi-direction to obtain sub-band coefficients by conducting contourlet transform. Then, by analyzing the coefficients, the appropriate fusion rules can be selected. The WRV rule was performed to fuse low frequency sub-band coefficients as the characteristics of low frequency sub-band mainly reflect the contour of an image. Additionally, the NHM rule was adopted to integrate high frequency sub-band coefficients which contain a lot of useful edge details of source images. Finally, an experiment based on computed tomography (CT) and magnetic resonance imaging (MRI) medical images was conducted. We also used evaluating indexes to verify the performance of the proposed algorithm. The simulated results show that the proposed method can extract features from source images and inject it into the ultimate object image, and evaluations can also prove that the method improves the blurring problem on edges and contours and promotes the performance of the algorithm.*

Subject Categories and Descriptors

H.2.8 [Database Applications]: Image database; **I.5.3 [Pattern Recognition]:** Algorithms

General Terms: Medical Imaging, Algorithm, Frequency Domain, Evaluation Indexes

Keywords: Digital image fusion, Medical image, Contourlet transform, Weighted regional variance, Neighborhood homogeneous measurement

Received: 10 January 2016, Revised 15 February 2016, Accepted 1 March 2016

1. Introduction

With the development of medical informatization, computer technology, and biomedical engineering, medical digital imaging equipment can enhance images with a variety of modalities for clinical diagnostics; these images provide important information regarding human organs and diseased tissue. Computed tomography (CT) imaging has high spatial resolution and preferable geometric properties, and can produce clear images of bones. So, CT can provide a good reference for the tumor localization; however, low contrast can often be found in detecting soft tissue. Magnetic resonance imaging (MRI) is capable of displaying anatomical structures, such as soft tissues, organs, and blood vessels, with high definition, which is conducive to determine the lesion scope, but is not sensitive to calcification and is apt to distort geometrically when magnetic interference occurs. Single photon emission computed tomography (SPECT) and positron emission tomography (PET) can obtain the distribution of radioactive concentration at any angle or section of the human body, and may reflect the metabolism

and blood flow conditions for tissues and organs and provide functional information. However, SPECT and PET cannot produce high resolution images; as a result, precise anatomic structures are difficult to obtain, as well as distinguished contouring of tissues and organs. As a result, morphological and functional information obtained from different digital imaging devices, regarding the same anatomical place of the human body, is mutual and complementary.

In clinical diagnosis, single modality images often fail to provide enough information for doctors; therefore, if multi-modality medical images can be fused appropriately, enabling anatomical and functional information to be combined organically, then it could be possible for doctors to make more precise decisions [1]. If multi-source information is displayed in a single digital image, doctors can understand the diseased tissue or organ more comprehensively, and they can then make a more accurate diagnosis or develop a more appropriate treatment.

2. State of the Art

Medical digital image fusion technology is a unique application in the information fusion field and is one of the medical digital image processing technologies developed from the 1990s. It combines a variety of medical image information and provides a new standard for modern clinical diagnosis. As an important image processing technology, medical digital image fusion has received wide attention in recent years. Chen et al. [2] discussed the value of target delineation of nasopharyngeal carcinoma (NPC) based on MRI / CT image fusion. The studies have shown that the MRI / CT image fusion improved the accuracy of gross tumor volume (GTV) delineation of NPC. Generally speaking, GTVs sketched by different doctors are often not the same due to the different physiological, psychological, and even cognitive statuses, and the accurate CT / MRI image fusion is more conducive to the implementation of precise radiotherapy. In studies of schizophrenia treatment, the early longitudinal studies did not show any change regarding the brain and caudate nucleus of the patient in CT images after diazepam medication. By using registration and fusion, Randy et al. [3] found that the caudate nucleus of five schizophrenic patients had atrophied during the past six-months, and the brain of another three patients had swelled. Additionally, these changes provide valuable references for diagnosing schizophrenia in different stages. Since the identification and diffusion of many tumors are not obvious and cannot be determined in anatomical images (CT or MRI), the best way to analyse tumors is to collect PET images with fluoro-deoxy-glucose (FDG) as tracer for now, so that the registration and fusion of PET, CT, and MRI images in tumor locating can provide references for surgery. Christian et al. [4] found that PET / MRI may further improve diagnostic accuracy in the differentiation of scar tissue from recurrence of tumors such as rectal cancer by fusing functional MRI to PET images. They also summarized the available first experiences with PET / MRI and outlined

the potential value of PET / MRI in oncologic applications. Liu et al. [5] developed a tumor locating system by fusing MRI / CT images and PET / CT images, and the volume method, gross target / common target methods were used to evaluate the changing of nasopharyngeal neoplasm GTV and lymph node GTV. The studies have shown that PET / CT fusion can be used to produce more accurate staging and a more suitable therapy plan and will influence the GTV definition further. Zhou et al. [6] discussed the application of CT / MRI image fusion in three-dimensional conformal radiotherapy GTV determination of primary liver cancer. Studies have shown that the use of CT / MRI image fusion technique was valuable for primary three-dimensional conformal radiotherapy GTV determination and can reduce the side effects on surrounding organs. Many other scholars have conducted related studies in the multi-modality image fusion domain, such as the wavelet based transform [7,8], the neural network based transform [9], fusion based on vision [10,11], fusion based on ridgelet [10], and other methods [11–14].

Image fusion technology consists of two parts: space domain and multi-resolution frequency domain [15]. Contourlet transform is a multi-resolution, localized and multi-directional image representation that inherits the scaling relation of anisotropy of curvelet transform, and it can be considered as a digital implementation to approximate the curvelet transform in a certain sense. Contourlet transform is a sparsely two-dimensional digital image representation with properties of directionality and anisotropy; it captures the contour information of images in sub-bands of different scales and different directions, and it can be applied in the field of digital image fusion effectively [16]. By studying digital image fusion and contourlet transform, this paper proposed a CT / MRI image fusion algorithm based on weighted regional variance (WRV) and neighborhood homogeneous measurement (NHM) rules in the contourlet domain.

The remainder of this paper is organized as follows: Section 3 shows how the low frequency and high frequency sub-bands are integrated and what indexes are used to evaluate images. In section 4, the experiments on contourlet decomposition are conducted, and then the performances of the different algorithms and similar algorithms with different fusion rules are both compared. Lastly, conclusions and future works are given in section 5.

3. Methodology

Perfect registration is the premise of image fusion, so a strict registration has been made before performing digital image fusion in this article. It is valuable to conduct image fusion only when the pixels of two medical images at the same spatial location are mapped to the same anatomical structure.

The structure is made up of a Laplace pyramid (LP) and directional filter banks (DFB), which perform the multi-scale analysis and multi-directional analysis, respectively

[17]. The contourlet transform approximates a digital image by using the stripe-like base structure which is similar to the contour segment and the base structure changes when different aspect ratios are used. Figure 1 shows the comparison between wavelet base and contourlet base when approximating a curve. The figure shows that contourlet has the property of directionality and anisotropy, demonstrates lines and surfaces of an image more sparsely. Usually, coefficients with larger values correspond to very few points of the image after implementing contourlet transform, and these points concentrate most of the information and energy of the image, so a reasonable fusion system must take these points with larger values into account when designing the fusion rules. Figure 2 demonstrates the profile of coefficient distribution of a test image under contourlet domain, which is unlike the regular distribution of two-dimensional wavelet decomposition. Additionally, the coefficient distribution of contourlet transform is related with the parameters produced by the pyramid directional filter banks (PDFB) in the whole decomposition process.

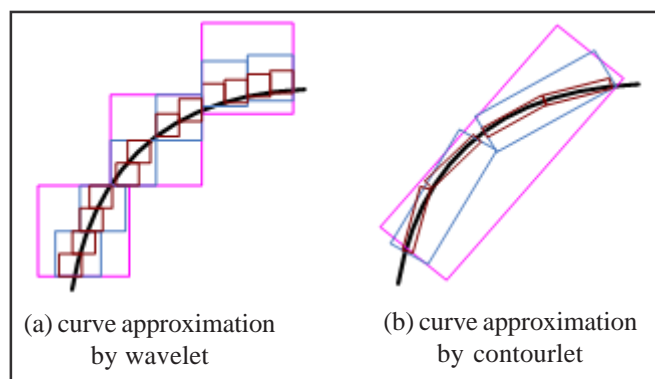


Figure 1. The difference of wavelet and contourlet bases approximate a curve

Given that the test medical digital images have been registered, the fusion steps for CT / MRI medical image based on WRV and NHM are shown as follows: 1) Perform multi-scale and multi-directional contourlet transform on the two source digital images, A and B , separately. Multi-scale decomposition using LP transform to capture singularities in the two-dimensional image must first be conducted. Then DFB decomposes the high frequency signals on each

scale and integrates singularities that distribute in the same direction of the specified coefficient. 2) Implement the fusion rules after analyzing the coefficients generated by contourlet transform, so the function of fusion rules for both low and high frequency sub-bands can be embodied in the optimization process. The low frequency sub-band contains the approximation of the original image, which accounts for the energy of the image. Therefore, for medical image fusion, it is possible to choose the suitable fusion rule only when the characteristics of different imaging modes have been analyzed. Coefficients with larger absolute values in high frequency sub-bands correspond to mutations, such as edge, texture, and other important information of the image. The main objective in handling the high frequency information is to increase the image detail as much as possible. So the WRV and NHM based fusion rules are designed for low and high frequency sub-bands, respectively. 3) Conduct inverse contourlet transform on integrated coefficients to obtain a fused image, and evaluate the image quality from subjective and objective aspects. The image fusion process is shown in Figure 3.

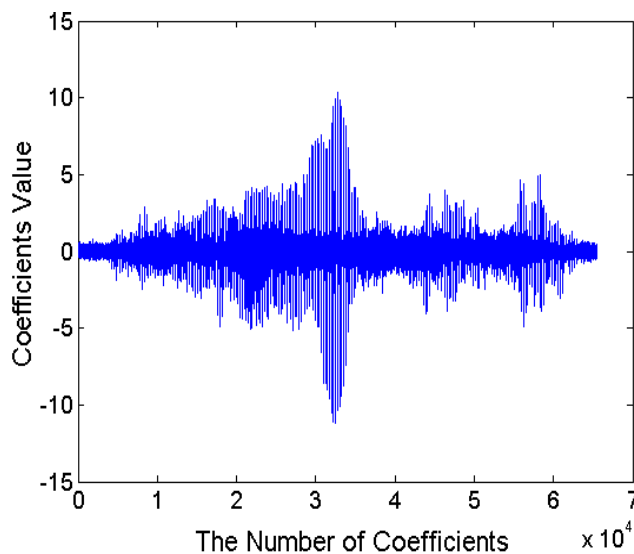


Figure 2. The distribution of contourlet coefficients after decomposition

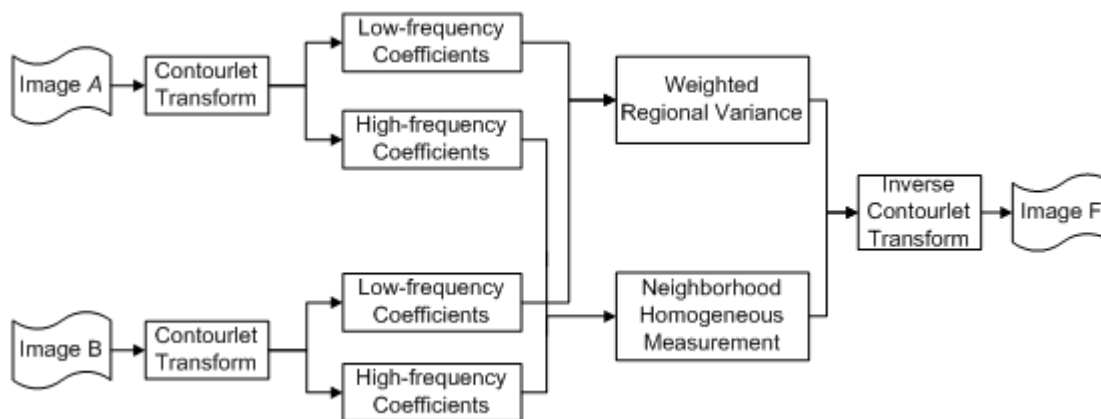


Figure 3. Flow chart for the fusion algorithm

3.1 Rules for Low Frequency Sub-band

The low frequency sub-band acquired from the contourlet domain mainly represents image contour. At present, the commonly used fusion rules for low frequency sub-band image are averaged pixel value, pixel extremum, and other related methods. The pixel extremum method includes two branches, maximum and minimum, which have the advantages of simple calculations and easy implementation. However, as the gray level of one source image is used as the gray value of the final image, in most cases, important medical information from other source images cannot be integrated, and sometimes distortions can also happen. The averaged pixel value method is made up of direct average and weighted-average, the averaging operation equates to performing smooth processing on images and generally makes the image blurred despite the fact that the method is effective in image fusion. Therefore, the average method blurs edges and contours of the fused image to varying degrees, and affects the overall contrast of the image; as a result, the regional characteristics of the pixel cannot be reflected accurately. Therefore, the WRV method is adopted to fuse low frequency sub-band coefficients in proposed algorithms, and the fusion details for low frequency sub-band coefficients are as follows:

Let $C_k(m, n)$ denote the coefficient at location (m, n) of the k^{th} image, where $k = 1, 2, 3$. The source digital images are A, B and the fused digital image is F ; $\mu_k(m, n)$ denote the mean of the 8-neighborhood region centers at position (m, n) ; and $sd_k^2(m, n)$ represent the variance of the 8-neighborhood centers at point (m, n)

$$\mu_k(m, n) = \frac{1}{9} \sum_{m=1}^3 \sum_{n=1}^3 C_k(m, n) \quad (1)$$

Suppose α is the weighted coefficient used in WRV for low frequency sub-band. Thus,

$$sd_k^2(m, n) = \frac{1}{9} \sum_{m=1}^3 \sum_{n=1}^3 (C_k(m, n) - \mu_k(m, n))^2 \quad (2)$$

and the fusion coefficient for low frequency sub-band at position (m, n) is $C_{\alpha}(m, n)$, which can be calculated as follows:

$$\alpha = \begin{cases} \frac{sd_A^2(m, n)}{sd_A^2(m, n) + sd_B^2(m, n)} \text{ (as } \alpha_1) & \text{if } sd_A^2(m, n) \geq sd_B^2(m, n) \\ \frac{sd_B^2(m, n)}{sd_A^2(m, n) + sd_B^2(m, n)} \text{ (as } \alpha_2) & \text{if } sd_A^2(m, n) < sd_B^2(m, n) \end{cases} \quad (3)$$

Compared with other fusion rules, the WRV proposed in the paper retains more sensitive information, as larger variance usually means more information is contained and the weighted coefficients in the algorithm extract sensitive information in a better way. So, this method is superior to the averaging approach as far as the fusion effect is concerned.

$$C_{\alpha}(m, n) = \begin{cases} C_A(m, n) \times \alpha_1 + C_B(m, n) \times \alpha_2 & \text{if } sd_A^2(m, n) \geq sd_B^2(m, n) \\ C_A(m, n) \times \alpha_2 + C_B(m, n) \times \alpha_1 & \text{if } sd_A^2(m, n) < sd_B^2(m, n) \end{cases} \quad (4)$$

3.2 Rules for High Frequency Sub-band

When the image is decomposed in contourlet domain, the high frequency sub-band coefficients embody particular information, edges, lines, and contours of the region. Additionally, the distribution of high frequency sub-band coefficients exhibit directional characteristics and contain detailed information for most of the images. For medical images, the high frequency sub-band coefficients are relatively stable and the contourlet coefficients are strongly correlated. The ultimate purpose of fusing high frequency sub-band coefficients is to retain clear details from source images as much as possible in order to keep more primitive medical information.

In this paper, a NHM based local self-adaptive fusion rule is adopted in high frequency sub-band coefficients fusion by calculating the level of similarity of the corresponding neighborhood to decide which coefficient is suitable for practical fusion, and the NHM can be calculated as follows:

$$NHM_{i,j}(m, n) = \frac{2 \cdot \left\{ \sum_{(k,l) \in N_{i,j}(m,n)} |C_{i,j}^A(m, n)| \cdot |C_{i,j}^B(m, n)| \right\}}{E_{i,j}^A(m, n) + E_{i,j}^B(m, n)} \quad (5)$$

where $E_{i,j}(m, n)$ represents the neighborhood energy under resolution of 2^j in direction i , and $N_{i,j}(m, n)$ represents the 3×3 neighborhood centers at point (m, n) . In fact, NHM quantifies the level of similarity of corresponding neighborhoods from source images, and a greater NHM value produces a higher similarity level. Because $0 \leq NHM_{i,j}(m, n) \leq 1$, we define a threshold T and generally have $0 < T < 1$. In our experiment, we set it as 0.75 experientially according to a series of tests; in these cases, the fused images have shown optimal results in visual effect and evaluation indexes. Therefore, the threshold is given as $T = 0.75$, and the fusion rule of high frequency sub-band coefficients are expressed as the following:

$$\begin{cases} C_{i,j}^F(m, n) = C_{i,j}^A(m, n) & \text{if } E_{i,j}^A(m, n) \geq E_{i,j}^B(m, n) \\ C_{i,j}^F(m, n) = C_{i,j}^B(m, n) & \text{if } E_{i,j}^A(m, n) < E_{i,j}^B(m, n) \end{cases} \quad \text{if } NHM_{i,j}(m, n) < T$$

$$C_{i,j}^F(m, n) = NHM_{i,j}(m, n) \cdot \max(C_{i,j}^F(m, n), C_{i,j}^A(m, n)) + (1 - NHM_{i,j}(m, n)) \cdot \min(C_{i,j}^F(m, n), C_{i,j}^B(m, n)) \quad \text{if } NHM_{i,j}(m, n) \geq T \quad (6)$$

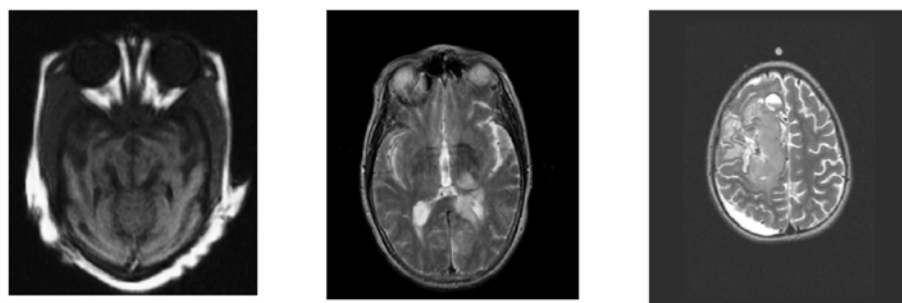
3.3 Quantified Evaluation Indexes

At present, the quantitative evaluation indexes for medical digital image mainly include three classes: evaluation based on the amount of information (class 1), evaluation based on statistics (class 2), and evaluation based on relevance (class 3) [17]. The indexes of class 1 include information entropy (IE), cross entropy (CE), and joint entropy (JE), etc. Class 2 contains mean (ME), standard deviation (SD), average gradient (AG), edge Q index (Q Index), peak signal to noise ratio (PSNR), mean square error (MSE), and root mean square error (RMSE), etc. Mutual information (MI), correlation coefficient (CC), and relative deviation (RD), etc. belong to class 3. In this paper, we select IE, SD, AG, Q Index, and MI as quantitative evaluation

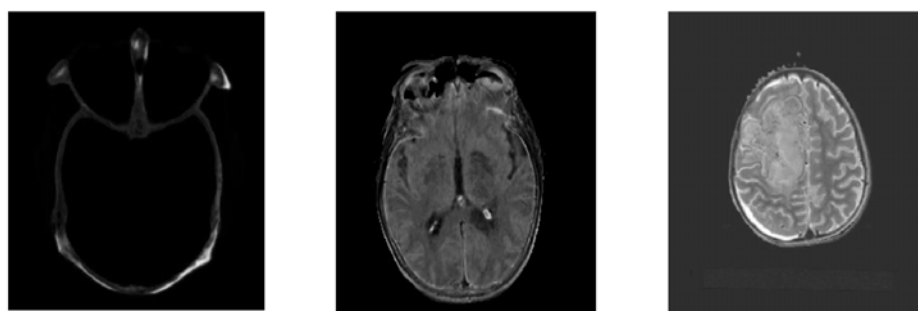
metrics. IE is one of the most widely used indexes, the value of which directly reflects the amount of information for an image. Larger IE value means that more information is contained in an image. SD indicates the level of deviation between the gray values of pixels and the average of the fused image. In a sense, greater fusion effect creates a greater SD. AG is capable of expressing the definition of the fused image, and the level of definition is better if there is a larger AG value of an image. MI measures the mutual dependence of the two random variables, so a better fusion effect produces a bigger MI. Q index measures the amount of edge information transferred from source images to the fused one, larger Q value indicates better algorithm performance.



(a) CT images



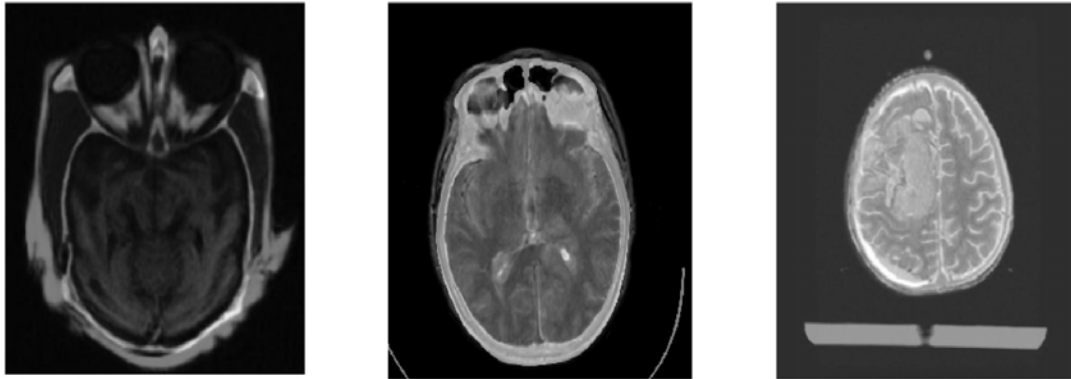
(b) MRI images



(c) Fused images based on minimum coefficient



(d) Fused images based on maximum coefficient



(e) Fused images based on average coefficient



(f) Fused images based on proposed WRV+NHM

Figure 4. Fusion results of four fusion rule in contourlet domain

4. Analysis of Results and Discussion

In our experiment, both CT and MRI images are selected to conduct fusion purpose in which two types of comparison are performed. Comparison 1 is implemented between different fusion rules in the contourlet domain, while comparison 2 is between contourlet transform and some other varied fusion methods.

In comparison 1, the minimum, maximum, average, and proposed WRV + NHM rules are adopted, respectively, in analyzing fusion performance. The fusion result of comparison 1 is shown in Figure 4, and Figures 4(a) and 4(b) are CT and MRI source images, respectively, and in each image row, three different images are chosen to identify the experiment. Figures 4(c), 4(d), and 4(e) represent the fused images by using minimum, maximum, and average coefficient rules in the contourlet domain, respectively, for low frequency and high frequency subbands fusion, and Figure 4(f) demonstrates the fused image performing proposed WRV + NHM fusion rules.

Figure 4 shows that all four fusion methods can extract information from both source images and eject it into the fused image. From a subjective point of view, Figure 4(c) produces three groups of slightly blurred and dim images when compared to Figures 4(d), 4(e), and 4(f). In particular, the first column of Figure 4 (c) fails to integrate most of

the information that comes from the MRI image, which implies that the minimum coefficient fusion rules are not applicable for medical image fusion tasks in contourlet domain in this article. Figure 4(d) shows the intensity of the images produced by the maximum coefficient fusion rule is enhanced relative to source images. As far as Figures 4(e) and 4(f) are concerned, images generated by average and proposed methods are superior to the other two methods both in definition and in the level of information abundance. As the subjective estimation is likely to be affected by psychological status and even mental states of the observer, the objective criteria must be used in fusion effect evaluation. In this paper, IE, SD, AG, Q Index, and MI are adopted to carrying out objective evaluation. Statistic results in Table 1 partly prove what we have seen in Figure 4 considering the limit of the paper length only data related to column 2 is listed.

Table 1 illustrates that the minimum coefficient rule may cause distortions for fused images during an experiment, as a result, the source information cannot be integrated. Both maximum and average fusion methods achieve better fusion effects when compared with the minimum approach. The proposed WRV + NHM method in contourlet domain outperforms the above mentioned three approaches in four of five criteria. Of them, the indexes, IE, AG, Q, and MI of WRV + NHM, exceed those of three methods (from top to bottom) by 69.0%, 19.0%, and 22.8% (for IE), 72.0

%, 13.7%, and 75.7% (for AG), 48.3%, 11.7%, and 52.4% (for Index Q), 63.8%, 32.8%, and 33.9% (for MI), respectively, and it is slightly inferior to maximum method only for SD. Therefore, the fused medical image created by the

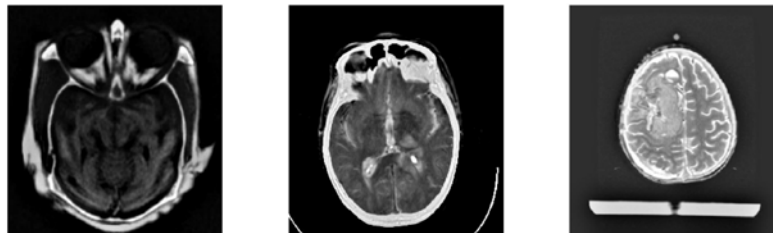
proposed method has richer information, expresses relatively high definition, and enjoys more edge details transferred from source images and a better fusion effect.

	IE	SD	AG	Q Index	MI
Minimum	3.2252	7.9243	0.0344	0.4549	3.2924
Maximum	4.5775	8.8872	0.0465	0.6038	4.0606
Average	4.4369	8.7263	0.0301	0.4426	4.0262
Proposed	5.4510	8.8207	0.0529	0.6746	5.3926

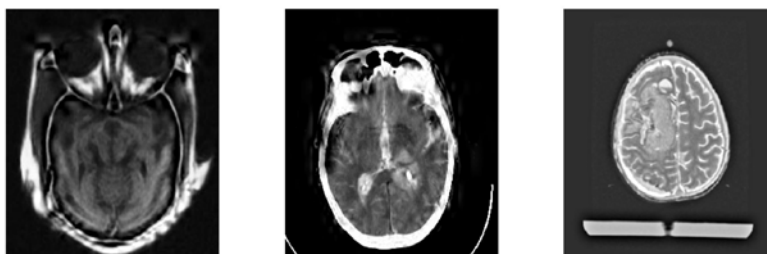
Table 1. Performance comparison for different fusion rules (data from column 2 of Figure 4)



(a) Fused images based on PCA



(b) Fused images based on LP



(c) Fused images based on wavelet

Figure 5. Fusion results of other three fusion methods

	IE	SD	AG	Q Index	MI
PCA	4.1907	8.7886	0.0327	0.4479	3.8615
LP	6.0160	8.7618	0.0544	0.6445	3.0866
Wavelet	5.4700	8.8215	0.0535	0.5431	2.9161
Proposed	5.4510	8.8207	0.0529	0.6746	5.3926

Table 2. Performance comparison of different fusion methods (data from column 2 of Figure 5)

In order to demonstrate the superiority of the proposed algorithm further, experiments on three other methods are performed in comparison 2. In this group of analysis, there are three different fusion algorithms adopted, including a statistics based method of principal component analysis (PCA), a multi-resolution decomposition based method of Laplace pyramid (LP) transform, and a wavelet based method. Figure 5(a) is the fusion result of PCA method, the basic principle of which is to obtain the principal components of medical source images with different modality by using PCA, then achieving the fusion image by conducting a weighted average method. Figure 5(b) is the fusion result of LP method, while the decomposition level is selected as 4 and highpass and lowpass sub-bands are treated by “choose max” and “average” rules, respectively. Figure 5(c) shows the fusion result of the wavelet, the number scale is set to 4, and the wavelet base is “haar.” Table 2 evaluates the fusion results obtained by four different methods; the PCA is based on statistics and the other three are based on transform domain. Experimental results show that the transform domain algorithms have more advantages than the former when fusing CT / MRI medical images.

5. Conclusions

To enhance algorithm efficiency and performance, an improved approach for medical digital image fusion based on weighted regional variance (WRV) and neighborhood homogeneous measurement (NHM) algorithm in contourlet transform domain was proposed in this paper. The source images were first decomposed in multi-scale and multi-direction using the contourlet transform. Then, the WRV and NHM fusion rules were adopted to get low-frequency coefficients and high-frequency coefficients, respectively. The ultimate fused image was achieved at last by integrating all obtained sub-band coefficients with the inverse contourlet transform. The main conclusions can be drawn as follows:

- 1) The contourlet transform has a comparative advantage in image fusion application field; it can be applied in CT and MRI medical image fusion, and a WRV+NHM fusion rule was also used in contourlet domain and achieved satisfied results.
- 2) The proposed WRV+NHM algorithm achieved desired CT / MRI fusion images when compared with the different fusion rules in contourlet domain and even the different fusion methods.
- 3) When compared to minimum, maximum, and average fusion rules in contourlet domain, the proposed method was superior to other three approaches in definition and obtained the highest evaluation values in information entropy, average gradient, edge Q index and mutual information.
- 4) When compared to principal component analysis (PCA), Laplace pyramid (LP), and wavelet fusion

methods, the statistics based method PCA were inferior to other three transform domain based methods. PCA got the last evaluation place, and it was difficult to determine which one of the three transform domain methods was the best in all medical image fusion tests. However, it was a useful and valuable attempt by employing WRV+NHM rule in contourlet domain to fuse medical images.

At present, there are still many technical problems that need to be solved when applying the proposed algorithm to clinical diagnosis, and how the proposed algorithm can be used to fused medical images with other modalities is an important step in our future work. As the fusion methods adopted in multi-modal medical image fusion can be different, how to establish a rational, optimized fusion system for multi-modal medical images is one of the key focuses for future studies.

Acknowledgment

This work was supported by National Breeding Project of China west normal university under grant number “13C003”.

References

- [1] Favazza, C., Gorny, K., Felmlee, J., et al. (2013). SU-E-I-68: preliminary evaluation of potential MRI contrast materials for the purpose of MR-ultrasound fusion application in the abdomen. *Medical Physics*, 40(6) 231-238.
- [2] Chen, J.W., Pan, J.J., Du, B.G., et al. (2009). Influence of CT-MRI fusion image on definition of the target volumes of nasopharyngeal carcinoma. *Tumor*, 29 (1) 61-64.
- [3] Randy, L.G., Jody, M.S., Margaret, D., et al. (2013). The MCIC collection: a shared repository of multi-modal, multi-site brain image data from a clinical investigation of schizophrenia. *Neuroinformatics*, 11(3) 367-388.
- [4] Christian, B., Till, A.H., Thomas, C.L., et al. (2012). Oncologic PET/MRI, part 1: tumors of the brain, head and neck, chest, abdomen, and pelvis. *The Journal of Nuclear Medicine*, 53(6) 928-938.
- [5] Liu, X.J., Chen, S.P., Zhang, X.Z., et al. (2013). Application of PET/CT image fusion for conformal radiotherapy in nasopharyngeal carcinoma. *Journal of Clinical Medicine in Practice*, 7(19) 41-43.
- [6] Zhou, Z.D., Shi, G.Y., Chen, R. (2013). Application of CT and MRI image fusion technique to determine the three-dimensional conformal radiotherapy in primary liver cancer. *China Practical Medicine*, 7(25) 84-85.
- [7] Bruno, A., Mario, C., Giuseppe, D. P. (2007). A wavelet-based algorithm for multimodal medical image fusion. *Lecture Notes in Computer Science, Springer Berlin Heidelberg*, 117-120.
- [8] Li, S.T., Yang, B. (2015). Multifocus image fusion by combining curvelet and wavelet transform. *Pattern Rec-*

ognition Letters, 29 1295-1301.

(9) 1295-1301[9] Nasrin, A., Fatemizadeh, E., Hamid, B (2014). MRI-PET image fusion based on NSCT transform using local energy and local variance fusion rules. *Journal of Medical Engineering & Technology*, 38 (4) 211-219.

[10] Chen, G.Y., Qian S.N., Jeanpierre, A., et al (2012). Super-resolution of Hyperspectral Imagery Using Complex Ridgelet Transform. *International Journal of Wavelets Multiresolution & Information Processing*, 10 (10) 1347-1361.

[11] Fourati, M., Jedidi, A., Hassin, H.B., et al (2015). Towards fusion of textual and visual modalities for describing audiovisual documents. *International Journal of Multimedia Data Engineering & Management*, 6 (2) 52-70.

[12] Bhatnagar, G., Wu Q.M.J., Liu, Z (2013). Directive contrast based multimodal medical image fusion in NSCT domain. *IEEE Transactions on Multimedia*, 15 (5) 1014-1024.

[13] Daneshvar, S., Ghassemian H (2010). MRI and PET image fusion by combining IHS and retina-inspired models. *Information Fusion*, 11 (2) 114-123.

[14] Karunanithi, S., Sharma, P., Kumar, A., et al (2013). 18 F-FDOPA PET/CT for detection of recurrence in patients with glioma: prospective comparison with 18 F-FDG PET/CT. *European Journal of Nuclear Medicine & Molecular Imaging*, 40 (7) 1025-1035.

[15] Xu, S (2011). Study of a medical image fusion algorithm based on contourlet regional statistics. *Chinese Journal of Medical Imaging Technology*, 27 (11) 2326-2330.

[16] Lebedeva, E.A., Postnikov, E.B (2014). On alternative wavelet reconstruction formula: a case study of approximate wavelets. *Royal Society Open Science*, 1 (2) 11-21.

[17] Wang, J., Lai, S.Y., Li, M.D (2012). Improved image fusion method based on NSCT and accelerated NMF. *Sensors*, 12 (5) 5872-5887.